Highlights of Neutronics Analyses for the Pre-conceptual NIST Neutron Source Design

Osman Ş. Çelikten, Dağıstan Şahin, Abdullah G. Weiss

NIST Center for Neutron Research, 100 Bureau Drive, Gaithersburg, MD 20899, USA
osman.celikten@nist.gov; dagistan.sahin@nist.gov; abdullah.weiss@nist.gov

doi.org/10.13182/T127-39593

INTRODUCTION

Preliminary efforts are currently underway towards the development of a replacement for the National Bureau of Standards Reactor (NBSR) at the NIST Center for Neutron Research. The replacement reactor, namely NIST Neutron Source (NNS), is a 20 MW light-water cooled and heavy & light-water moderated compact core reactor. The NNS design builds on a previous replacement reactor concept to replace the NBSR [1]. Of interest to this paper are the neutronics analyses conducted using Monte Carlo N-Particle (MCNP) code [2], which are used to determine neutronic characteristics such as kinetics, power and fission density of the core across multiple cycles and operating states.

This paper describes the core geometry and discusses some preliminary results for power peaking calculations and fission density distributions at multiple cycle operation states. These states of operation are startup (SU), beginning of cycle (BOC), middle and end of cycle (MOC and EOC, respectively).

METHODOLOGY

The proposed core, shown in Fig. 1, is composed of nine fuel assemblies and two cold neutron sources on either side of the core per Fig. 2. Each fuel assembly contains 21 U-10Mo fuel plates which are 19.75% enriched Y-12 fuel wrapped with ~8 μm thick zirconium foil to prevent fuel-clad chemical interactions with the Aluminum-6061 cladding [3-4]. The core is designed to optimize the length of the fuel cycle while maintaining a negative power reactivity feedback within a compact core (minimal footprint).

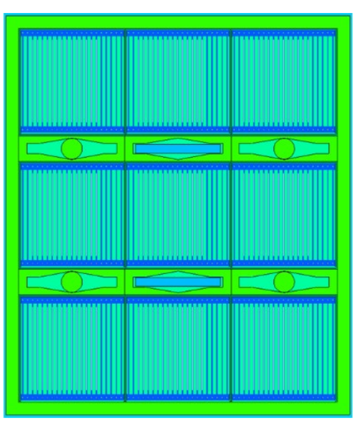

Fig. 1. The pre-conceptual core design for the NNS

Note the presence of 2 control blades surrounding the central fuel assembly, and 4 safety blades to separate each row of fuel assemblies. The configuration shown here reflects the axial center of the core. Both control and safety blades are made of hafnium, which is selected for its increased longevity relative to cadmium blades. In order to suppress the higher flux of the reactor at the initial stages of the fuel cycle, 2 cadmium wires (0.5 mm diameter) are placed on each radial side of each fuel plate. The cadmium wires slide into H_2O-filled T-shaped slots within the side plates of each assembly, where the water is used to provide some level of cooling for the cadmium wires. In the model, the fuel meat in each plate is discretized into axial and radial zones to account for spatial variations in the reactor neutron density distribution and fuel composition. Axially, the fuel meat is discretized into 10 zones, where the top and bottom zones are 2 cm high while the rest are 8.25 cm high. Radially, the fuel is uniformly discretized into 3 zones with a width of 2.167 cm. The thickness of the fuel plates is 0.25 mm.

The power and fission densities for a given core spatial position was calculated by using MCNP6. It is conservatively assumed that all recoverable fission energy deposited within the selected volume, and the power and fission densities are directly proportional to the fission energy deposition. Each fuel meat in the plates is divided into 30 sections as described before. Consequently, the local power densities are the result of multiplication of local peaking factors and the average power densities [5-6].

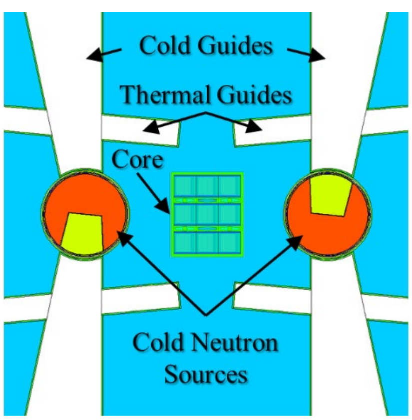

Fig. 2. A top view of the NNS core and cold neutron sources.

The NNS is designed to be a high leakage core, so that it can service neutron scattering and irradiation experiments via out-of-core neutron guides. For neutron scattering experiments in particular, cold neutrons (wavelengths > 4 Å) are more useful, and they can be obtained using the cryogenically cooled liquid deuterium-filled cold sources on either side of the core. Connected to the cold sources are cold neutron guides made of zirconium alloy. Thermal neutron guides, also made of zirconium, extend to near the core and allow for out-of-core thermal neutron experiments. The presence of the cold neutron sources and the neutron guides are important to understand the behavior of the core, and as such, they are included in this work's MCNP models.

RESULTS

The power peaking at each fuel plate throughout the core is shown in Fig. 3 at multiple cycle states, where the view and orientation of the core is aligned with Fig. 1. The average power generated in each assemblies is 2.22 MW and the maximum generated power is calculated as 2.518 MW. The highest power peaking occurs near the outer edges of the assemblies throughout all cycle states hence relatively higher moderation is observed at the peripheral side of the cores. An assembly power of 2.367 MW and a 1.77 power peaking factor is obtained for the hottest plate for SU. The results show that the outside plates have more power than the inner plates due to increased moderation (water) being present at the edges.

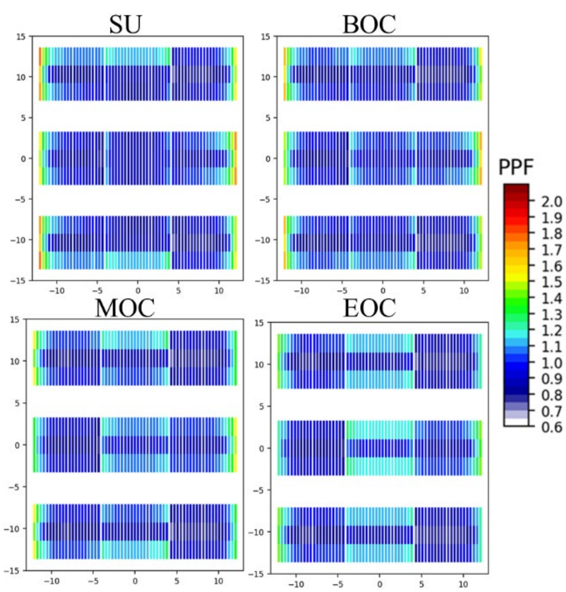

Fig. 3. A spatial distribution of the power peaking factors at each fuel plate throughout the core.

Next, using the implemented spatial discretization, the power and fission densities at each node throughout the model (19,845 total nodes) are obtained and plotted at multiple cycle states and multiple cycles such that each cycle spans 40 days. These power and fission densities are illustrated in Fig. 4 (a) for cycles 1-3 and Fig. 4 (b) for multiple cycle states. Note the presence of two additional cycle states in Fig. 4 (b), where the quarter 2 (Q2) and quarter 4 (Q4) states are used to cover the 2nd and 4th quarters of the 40-day cycle, respectively. Those two states are used to eliminate possible errors that could arise from the constant location of control blades while moving from BOC to MOC or from MOC to EOC, respectively.

The lower fission densities in the 1st cycle are due to the freshly loaded cadmium absorber wires, which effectively suppress the flux in those early stages of operation. As the cadmium burnable poison is utilized, the power density grows from ~16 kW/cm^3 in the 1st cycle to ~18 kW/cm^3 in the 3rd cycle. The fission density similarly grows from ~1.5×10^{21} cm^{-3} to ~4.4×10^{21} cm^{-3} as operation progresses from the 1st to 3rd cycle.

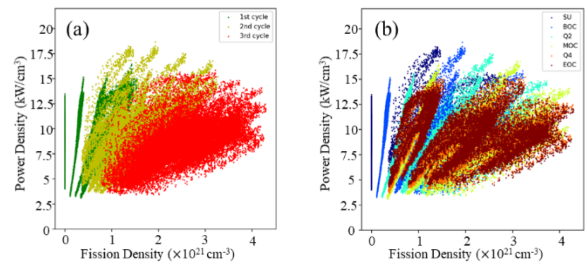

Fig. 4. A distribution of the correlation between power and fission densities throughout the core at (a) multiple cycles and (b) multiple cycle states.

To get a better understanding of how NNS compares to other U.S. high-performance research reactors (USHPR), Fig. 5 shows the comparison of the power and fission densities range (represented by the shapes) of NNS in comparison to other reactors like the NBSR, the advanced test reactor (ATR), and university reactors at the university of Missouri (MURR) and the Massachusetts institute of technology (MITR) [7-8].

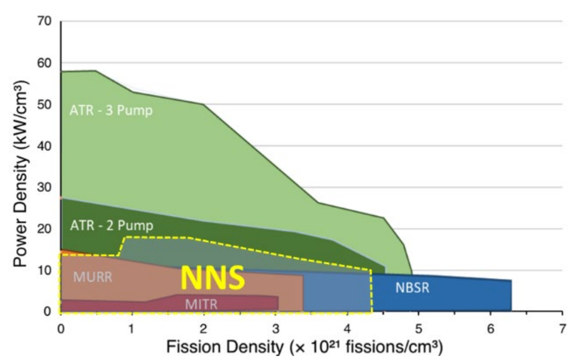

Fig. 5. The Power and fission density profile of the NNS compared to other high-performance research reactors (modified and reproduced from [7-8]).

ATR in 3 pump operation and the NBSR almost fully bound all other reactors, and as such represent the power density and fission density bounds, respectively. The region contained within the yellow dashed lines represents a preliminary estimate of the NNS operational envelope, where higher power density is afforded at lower fission density with respect to the NBSR. This demonstrates that NNS provides a very typical USHPR behavior when compared to other cores and is closer to ATR in operation envelope than it is to NBSR due to the elevated power density.

CONCLUSIONS

This work highlights the preliminary neutronics analysis conducted to characterize the behavior of the NNS at multiple cycle states of operation. An MCNP model is developed, and preliminary power peaking spatial distributions were obtained, revealing the highest power concentration near the edges of the core. Power and fission density correlations demonstrated the effectiveness of the cadmium burnable poison and revealed that NNS is closer in its operation envelope to the ATR. Further studies are currently being pursued to assess the equilibrium cycle behavior and better understand reactivity feedback and kinetics parameters. We will present our methodology in development of the MCNP model for the NNS and available results for the neutronic analyses.

ACKNOWLEDGEMENTS

The authors would like to acknowledge Robert E. Williams from the NCNR and David J. Diamond from Brookhaven National Laboratory for their helpful discussions.

DISCLAIMER

Certain commercial equipment, instruments, or materials are identified in this study in order to specify the experimental procedure adequately. Such identification is not intended to imply recommendation or endorsement by the National Institute of Standards and Technology, nor is it intended to imply that the materials or equipment identified are necessarily the best available for the purpose.

REFERENCES

1. T. Newton, D. Turkoglu, D. Diamond, L. Cheng, “Comparison of LEU Fuel Designs for the NBSR and a Replacement Reactor Concept,” *Trans. Am. Nucl. Soc*., **123**, 319–321 (2020).
2. C.J. Werner, “MCNP User’s Manual - Code Version 6.2”, Los Alamos National Laboratory, LA-UR-17-29981 (2017).
3. O.S. Celikten, D. Sahin, “The Effects of Impurities in Down-Blending Highly Enriched Uranium on the Reactor Neutronics and Cycle Length,” *Trans. Am. Nucl. Soc*., **125**, 165–167 (2021).
4. A. B. Robinson, G. S. Chang, J. Keiser, D. M. Wachs, and D. L. Porter, “Irradiation Performance of U-Mo Alloy Based ‘Monolithic’ Plate-Type Fuel – Design Selection,” Idaho National Laboratory, INL/EXT-09-16807 (2009).
5. Z. Wu and R. E. Williams, “Reactor Power Distribution Calculation in Research Reactors Using MCNP,” *Trans. Am. Nucl. Soc*., **113**, 1171-1174 (2015).
6. Z. Wu et al., “Neutronics and Safety Studies on a Research Reactor Concept for an Advanced Neutron Source,” *Nuclear Technology* **199** 1, 67 (2017)
7. J. Stevens and E. Wilson, “Progress on U.S and International Low-Enriched Uranium Reactor Conversions,” *Trans. Am. Nucl. Soc*., **123**, 311–314 (2020).
8. D. Jaluvka, E. Wilson, L. Jamison, and J. Stillman, “Experiment and Design Integration for U.S. High Performance Research Reactor Low-Enriched Uranium Conversion,” *Trans. Am. Nucl. Soc*., **123**, 359–362 (2020).